HHS Public Access

Author manuscript

J Comp Neurol. Author manuscript; available in PMC 2015 November 30.

Published in final edited form as:

J Comp Neurol. 1995 May 29; 356(2): 275–287. doi:10.1002/cne.903560210.

Octopamine Immunoreactivity in the Fruit Fly *Drosophila melanogaster*

MARIA MONASTIRIOTI, **MICHAEL GORCZYCA**, **JÜRGEN RAPUS**, **MANFRED ECKERT**, **KALPANA WHITE**, and **VIVIAN BUDNIK**

Department of Biology, Brandeis University, Waltham, Massachusetts 02254 (M.M., K.W.); Institut für Allgemeine Zoologie und Tierphysiologie, Biologische Fakultät, Friedrich-Schiller-Universität. D-07743 Jena, Germany (J.R., M.E.); Department of Biology, Morrill Science Center, University of Massachusetts, Amherst, Massachusetts 01003 (M.G., V.B.)

Abstract

Octopamine has been proposed as a neurotransmitter/modulator/hormone serving a variety of physiological functions in invertebrates. We have initiated a study of octopamine in the fruit fly *Drosophila melanogaster*, which provides an excellent system for genetic and molecular analysis of neuroactive molecules. As a first step, the distribution of octopamine immunoreactivity was studied by means of an octopamine-specific antiserum. We focused on the central nervous system (CNS) and on the innervation of the larval body wall muscles. The larval octopamine neuronal pattern was composed of prominent neurons along the midline of the ventral ganglion, whereas brain lobes were devoid of immunoreactive somata. However, intense immunoreactive neuropil was observed both in the ventral ganglion and in the brain lobes. Some of the immunoreactive neurons sent peripheral fibers that innervated most of the muscles of the larval body wall. Octopamine immunoreactivity was observed at neuromuscular junctions in all larval stages, being present in a well-defined subset of synaptic boutons, type II. Octopamine immunoreactivity in the adult CNS revealed many additional neurons compared to the larval CNS, indicating that at least a subset of adult octopamine neurons may differentiate during metamorphosis. Major octopamine-immunoreactive neuronal clusters and neuronal processes were observed in the subesophageal ganglion, deutocerebrum, and dorsal protocerebrum, and intense neuropil staining was detected primarily in the optic lobes and in the central complex.

Keywords

octopamine neuron; insect nervous system; neuromuscular junction; synaptic bouton; immunocytochemistry

Biogenic amines as chemical messengers in the nervous system of arthropods are thought to play crucial roles in several aspects of their behavior (reviewed by Bicker and Menzel, 1989). Octopamine, one of the biogenic amines extensively studied in invertebrates, has been proposed as neurotransmitter, neuromodulator, and neurohormone in a variety of physiological processes (for reviews, see David and Coulon, 1985; Evans, 1985, 1992;

Address reprint requests to Dr. Maria Monastirioti, Department of Biology, Brandeis University, Waltham, MA 02254..

Bicker and Menzel, 1989). In crustaceans, octopamine has been implicated in the neuromodulation of rapid response circuits controlling the escape behavior of crayfish (Glanzman and Krasne, 1983) and in the aggressive and submissive postures in lobsters (reviewed by Kravitz, 1988). In a variety of insect species, octopamine has been implicated in both central and peripheral neural functions. It stimulates activity of the firefly light organ (Nathanson, 1979), induces flight motor activity, and acts as neurotransmitter/modulator in the locust central nervous system (CNS; Sombati and Hoyle, 1984). Octopamine regulates hormone release in cockroaches (Downer et al., 1984), induces lipid and carbohydrate metabolism in crickets (Fields and Woodring, 1991), and modulates feeding behavior of blowflies (Long and Murdock, 1983) and bees (Bicker and Menzel, 1989; Braun and Bicker, 1992). Additionally, both somatic and visceral muscles are innervated by octopamine-containing endings in several insect species (see, e.g., Hoyle et al., 1980). Physiological studies indicate that octopamine has excitatory modulatory actions at these muscles (Hoyle, 1984; Hidoh and Fukami, 1987; Malamud et al., 1988).

Initially, biochemical studies were used to determine the presence of octopamine in ganglia and in individual neurons in lobsters (Evans et al., 1976; Livingstone et al., 1981). In insects, octopamine has been detected biochemically in a subset of well known dorsal unpaired median (DUM) neurons of the ventral nerve cord (reviewed by Evans, 1985). Moreover, neutral red, which stains octopamine and other biogenic amines, in combination with the Falck-Hillarp technique, which stains catecholamines and serotonin (5-HT) but not octopamine, has been used to determine the location of putative octopamine-containing neurons (reviewed by Evans, 1985). Certain octopaminergic DUM neurons have also been revealed by the sulphide silver-staining method, which detects endogenous copper, a cofactor of the octopamine biosynthetic enzyme tyramine β-hydroxylase (Siegler et al., 1991). Recently, antibodies highly specific to octopamine have been developed that facilitate more definitive mapping of octopaminergic neurons in the nervous systems of several animals (Konings et al., 1988; Eckert et al., 1992; Stevenson et al., 1992; Schneider et al., 1993).

In *Drosophila melanogaster*, there is good evidence that the amines octopamine, 5-HT, and dopamine are utilized in the nervous system (reviewed by Restifo and White, 1990). For example, electrophysiological studies suggest effects of octopamine on the adult neuromuscular junction (Dudai et al., 1987). Binding studies using fly head homogenates and radiolabeled ligand indicate the presence of high-affinity octopamine binding sites in the fly head that exhibit pharmacological properties of the mammalian adrenergic receptors (Dudai and Zvi, 1984). Recently, molecular studies have identified and characterized a putative octopamine/tyramine receptor (Arakawa et al., 1990; Saudou et al., 1990), and cloning of a gene that putatively encodes tyramine β-hydroxylase has been reported (White and Monastirioti, 1993). Thus, it is likely that molecular genetic tools that will allow in vivo manipulations of the components of octopaminergic function will be available in the near future. However, at the anatomical level, there is no concrete information on the octopamine neurons, their location in the nervous system, or the sites of octopaminergic innervation. This situation is in contrast to the case with serotonergic and dopaminergic neurons, which are well-characterized neuronal subsets (Beall and Hirsh, 1987; Konrad and Marsh, 1987;

Budnik and White, 1988; Vallés and White, 1988). Previously, an additional set of neurons in the larval nervous system, the “novel-CF” neurons, were revealed when larval CNSs were incubated in exogenous L-dopa or dopamine. These neurons are distinct from the serotonergic and dopaminergic neurons and were suggested to be octopamine-containing neurons (Budnik et al., 1986).

Identification of octopamine-containing neurons and putative sites of octopaminergic innervation would indicate the regions/functions in which octopamine is required, thus contributing to the knowledge of the diverse physiologcal roles of this amine in insects. Moreover, knowing the octopamine neuronal pattern would facilitate the identification of genes involved in its biosynthetic pathway and their further molecular characterization. In this report, we use an antiserum highly specific for octopamine (Eckert et al., 1992) to locate the octopamine-immunoreactive (OA-IR) cell bodies and OA-IR neuropil regions in the adult and larval CNS. To determine if octopamine is present at neuromuscular junctions, we have examined the muscles of the larval body wall, a preparation composed of identifiable muscle fibers that are readily accessible for anatomical studies. We have identified OA-IR nerve terminals in these muscles and have traced them through the three larval developmental stages.

MATERIALS AND METHODS

Fly cultures

Flies were raised at 25°C on standard medium. For all preparations, a wild-type strain, Canton-Special, was used.

Immunocytochemistry

The anti-octopamine antiserum employed in this study was raised in rabbits immunized with DL-octopamine (Sigma, St. Louis, MO) conjugated to bovine thyroglobulin with glutaraldehyde, and its specificity was characterized by dot blot immunoassay. A detailed description of the antiserum preparation procedure and the specificity tests was given by Eckert et al. (1992). Two other anti-octopamine antisera were used for neuromuscular junction staining that were raised in the laboratory of Dr. E.A. Kravitz (Harvard University) and provided to us courtesy of Drs. H. Keshishian (Yale University) and G. Wyse (University of Massachusetts).

Octopamine immunoreactivity (IRy) was studied in the adult and larval CNS and in larval body wall muscles. For the CNS preparations, indirect immunofluorescence and indirect peroxidase methods were performed. It is important to note that immunodetection with the octopamine antisera required glutaraldehyde fixation and that the intensity of the signal was highly dependent on glutaraldehyde concentration. We found, for example, that the glutaraldehyde concentration required for CNS preparations substantially weakened the signal at the neuromuscular junction but that a lower glutaraldehyde concentration resulted in a robust signal at the body wall muscles (see below). This difference may be due to ease of penetration of the fixative in the various tissues.

Dissection and fixation

Adult CNS: Male and female flies were cooled for 15–30 minutes, then heads and bodies were fixed for 2 hours at 4°C [30 ml saturated aqueous picric acid solution, 10 ml 25% glutaraldehyde (6.26%), 0.2 ml glacial acetic acid (0.5%), and 1% sodium metabisulfite]. Brains and thoracicoabdominal ganglia were then dissected and postfixed for 1–2 hours in the above-described fixative.

Larval CNS: CNSs from third-instar larvae were dissected in ice-cold, Ca^{2+}-free *Drosophila* Ringer's solution (Budnik et al., 1986) and were fixed in ice-cold fixative (above) for 3–4 hours.

Body wall muscles: Body wall muscles were dissected in ice-cold Ca^{2+}-free EGTA saline (Budnik and Gorczyca, 1992) and were fixed for 3 hours in freshly prepared 1% glutaraldehyde and 1% sodium metabisulfite in 0.1 M phosphate buffer (pH 7.4).

Staining protocols—*CNS* All steps were performed at 4°C unless otherwise specified. After fixation, samples were washed (five or six times for 15 minutes each) in 0.1 M phosphate buffer, pH 7.5, 150 mM NaC1, and 1% sodium metabisulfite (PBS-S); reduced in 0.5% sodium borohydrate in PBS-S at room temperature for 20–30 minutes; washed twice (20 minutes each) in PBS-S and twice (30 minutes each) in PBS-S containing 0.3% Triton X-100 (PBS-SX). The washes were followed by preincubation with 2% goat normal serum for 1–2 hours or overnight and by incubation in the antioctopamine antiserum (1:1,000 in PBS-SX) for 24 hours. Samples were then washed for 3–4 hours in PBS-X and were incubated overnight in biotinylated goat anti-rabbit IgG (Vector Laboratories, Burlingame, CA) at a dilution of 1:100 in PBS-X. Washes (six times for 30 minutes each) were followed by an overnight incubation with a horseradish peroxidase (HRP)-conjugated avidin-biotin complex (Vectastain ABC; Vector). Samples were then washed in PBS-X for 30 minutes; PBS for 30 minutes; and 0.1 M Tris buffer, pH 7.6, for 30 minutes and incubated for 20 minutes at room temperature in 0.5 mg/ml of 3,3′-diaminobenzidine-tetrahydrochloride (DAB) in Tris buffer. The peroxidase reaction was initiated by addition of 0.005% hydrogen peroxide and was terminated by a water rinse after sufficient brown color had developed. Alternatively, we used a Cy3-conjugated, affinity-purified goat anti-rabbit IgG serum (Jackson Immunoresearch Labs) as secondary antibody diluted at 1:20 in PBS-X. After several washes in PBS-X and a final wash in PBS, the samples were mounted in Vectashield (Vector).

Samples for paraffin sectioning were dehydrated in an ethanol series and were embedded in Paraplast. Serial sections 5–7 μm thick were cut, deparaffinized, and mounted in Permount. Samples for whole-mount immunocytochemistry were dehydrated, cleared in methylsalicylate, and mounted in Permount. Fourteen adult heads, 6 adult thoracic, and 17 larval CNS preparations were analyzed for OA-IR ncuronal patterns.

To test the specificity of the antibody, we preincubated the antiserum (1:1,000) with 5×10^{-3} M DL-octopamine from Sigma at 4°C for 24 hours (Schneider et al., 1993). Control larval CNSs were then incubated with preabsorbed primary antibody and were processed as described above. No OA-IRy was observed in tissues incubated with preabsorbed antiserum.

Additionally, incubations in the Cy3-conjugated secondary antibody alone resulted in no staining. Moreover, control tissues that were incubated only in the biotinylated secondary antibody and processed according to the indirect peroxidase method (see above) also showed no staining.

Body wall muscles: After fixation, body wall muscle preparations were washed twice in PBS-S, treated in 0.1% $NaBH_4$ for 45 minutes at room temperature, washed once in PBS-SX, and incubated overnight in anti-octopamine antiserum diluted at 1:1,000 in PBS-SX. Samples were then washed three times in PBS-SX, incubated in Cy3-conjugated anti-rabbit IgG (1:20) for 2 hours, washed three times in PBS-X, and mounted in Vectashield. HRP immunocytochemistry of the body wall muscles was carried out according to Budnik and Gorczyca. (1992).

Analysis of larval body wall muscles was based on 27 third-instar, six second-instar, and eight first-instar preparations. The presence of OA-IRy in each of the 30 body wall muscles was assessed in detail in eight preparations (96 hemisegments, abdominal segments 2–7).

Samples were observed under epifluorescence on a Zeiss Axioskop or on a Biorad MRC600 confocal unit attached to a Nikon microscope. Confocal images were processed using NIH Image (version 1.5) and were photographed from the computer screen.

RESULTS

Distribution of OA-IRy in the larval CNS

The larval CNS consists of mature functional neurons as well as neuroblasts and their immature progeny, which are precursors of the adult-specific neurons. The CNS occupies the anteroventral region of the larval body and is a fused ganglion composed of the paired brain hemispheres and the composite ventral ganglion. In the brain hemispheres, the medial portion of the brain is flanked by the large anlage of the optic lobes. The ventral ganglion is a fusion of the subesophageal, three thoracic (prothoracic, mesothoracic, and metathoracic), and eight abdominal neuromeres.

OA-IRy was studied in larval whole-mount and serially sectioned CNS preparations (Figs. 1, 2). The most striking features of the OA-IRy were as follows: 1) All OA-IR neurons were located on the midline or in close proximity to it as single cells, pairs, or clusters; 2) OA-IR varicosities were observed throughout the neuropil of the ventral ganglion; and 3) there were no OA-IR somata in the brain hemispheres despite the profuse IR varicosities seen in some of their neuropil regions. A diagrammatic representation of all IR neurons and neuropil regions consistently observed is provided in Figure 1D, and a description of the approximate location and number of the IR neuronal somata is given in Table 1. In Figures 1A and 2A, the most intensely stained neuronal cluster can be seen; this was located in the subesophageal ventral cortex and was composed of about 10–14 cells (SM, subesophageal medial). The arrangement and morphology of the SM neurons can be appreciated readily in the sagittal section shown in Figure 2A. The cell bodies were localized in the ventral cortex, and the processes projected up to the dorsal neuropil regions. In the posterior ventral region of the subesophageal ganglion, two pairs of OA-IR neurons were also detected followed by

three additional pairs of OA-IR neurons (one per neuromere) flanking the midline (PM, paramedial; Fig. 1A, 2C). Along the ventral midline, a row of weakly OA-IR cells was observed in the abdominal ganglion (AM, abdominal medial; Figs. 1C, 2C). These cells were irregularly shaped, and, in whole mounts, the immunofluorescence staining had a granular appearance. In sagittal sections, the IR processes of the AM neurons followed an ascending route towards the dorsal neuropil (Fig. 2B). For each segment, two parallel fibers were observed, suggesting the existence of two cells per segment (arrow, Fig. 2B). Moreover, we observed two OA-IR axons exiting through the segmental nerves (Fig. 3A), suggesting that each of the two parallel fibers bifurcates at the dorsal neuropil. The OA-IR fibers observed in the nerves could not be traced back to the somata, but some of these fibers could be followed to the muscles of the larval body wall (see below).

Intense OA-IRy was also seen in the neuropil of the ventral ganglion and brain lobes. A network of highly IR longitudinal fibers was observed along both sides of the ventral ganglion midline extending anteriorly into the median region of the brain (Figs. 1, 2A,B). In the anterior region of the brain lobes, transverse OA-IR fibers connected the two OA-IR neuropil areas. In addition, OA-IR fibers forming a dense tract extended from the OA-IR medial brain neuropil and projected laterally, forming IR neuropil foci near the medial boundary of the optic lobes (Fig. 1B).

Innervation of body wall muscles by octopamine-containing endings

The abdominal body wall muscles of *D. melanogaster* larvae consist of 30 muscle fibers per hemisegment (see Fig. 5) arranged in a regular pattern (Crossley, 1978). Each muscle fiber is innervated by one or more motor neurons in a muscle specific manner (reviewed in Keshishian et al., 1993). Innervation of the body wall muscles is provided by three nerves; the intersegmental nerve (ISN), which innervates dorsal muscles 1–4, 9–11, and 18–20; the segmental nerve (SN), which, in the larval stages, is fused with the ISN nerve and which innervates muscles 5–8, 12–17, 21–24, and 26–29 (Johansen et al., 1989); and the transverse nerve (TN), which innervates muscle 25 (Gorczyca et al., 1994).

As in many insect muscles, the body wall muscles are innervated by multiple synaptic boutons, the sites of accumulation of synaptic vesicles and of neurotransmitter release (Jan and Jan, 1976; Atwood et al., 1993; Jia et al., 1993). Several types of synaptic terminals can be distinguished by their synaptic bouton morphology, the muscle region innervated, type of synaptic vesicles, and putative neurotransmitters. The large type I boutons (4–8 μm), which are restricted to the medial aspect of muscle fibers, appear to innervate all body wall muscles, whereas type II boutons (1–2 μm) are present along endings that extend the length of the muscle fiber of most muscles (Johansen et al., 1989; Budnik and Gorczyca, 1992). A third class of synaptic boutons is present only on restricted groups of muscles (Anderson et al., 1988; Cantera and Nassel, 1992; Gorczyca et al., 1993).

Octopamine-IR varicosities were found in the fused SN/ISN, whereas the TN was devoid of staining. Two labelled axons projected from each hemisegment of the ventral ganglion (Fig. 3A) and continued down the nerve to the body wall (Fig. 3B). After branching repeatedly, OA-IR terminals innervated most body wall muscles of thoracic and abdominal segments (Figs. 3, 4). In this study, we centered on the innervation of muscles in abdominal segments

2–7. Based on the size of IR boutons, the distribution of boutons on each muscle fiber and the specific muscles that they innervated, we concluded that OA-IRy was found in all type II terminals. Figure 4A shows ventral longitudinal muscles 6, 7, 12, and 13 stained with anti-HRP antiserum, which stains all bouton types (Johansen et al., 1989; Budnik et al., 1990). Muscles 12 and 13 show profuse innervation by type I and type II boutons, whereas muscles 6 and 7 are innervated by type I boutons only. Octopamine-IRy was found in muscles 12 and 13 but was absent in muscles 6 and 7 (Fig. 4B). Figure 4C shows OA-IRy in type II terminals on other body wall muscles.

Our results of OA-IRy at type II boutons were confirmed with two other anti-octopamine antisera from different rabbits (see Materials and Methods), although the staining with these anti-bodies was weaker and gave higher background (data not shown).

Figure 5 is a diagrammatic representation of all 30 abdominal muscles per hemisegment and indicates the frequency of OA-IR terminals at each muscle. Of the 30 muscles, 20 showed OA-IRy in 70–100% of the hemisegments analyzed (n = 96 hemisegments; muscles 1, 2, 8–16, 18, 19, 21–24, 26, 27). On three muscles, 17, 20, and 29, OA-IRy was detected in only 45–65% of the hemisegments analyzed. Only seven muscles (3–7, 25, and 28) were rarely (< 25%) innervated by OA-IR terminals. No segmental differences in the pattern of distribution of OA-IRy were found.

During the larval period the number and position of body wall muscles remain constant. However, accompanying the overall growth of the larva, a dramatic increase (about 100-fold in volume) in the size of each muscle fiber is observed. Previous studies have demonstrated that the growth of the muscle fibers is paralleled by a continuous expansion of the neuromuscular junction (Gorczyca et al., 1993) as well as by an increase in the number and size of synaptic boutons and an elongation of synaptic terminals. We investigated whether a similar expansion was observed in OA-IR endings during the larval stages. As expected, we found that very few OA-IR boutons were present in just-hatched larvae (Fig. 4D). While the muscles became larger during the second and third larval instars, OA-IR endings increased in number and overall size (data not shown).

Distribution of OA-IRy in the adult CNS

The CNS of *D. melanogaster* is organized as a peripheral cortex, composed of neuronal cell bodies, that surrounds the neuropil. The brain neuropil consists of aggregates of fibers with characteristic, recognizable shapes (e.g., mushroom bodies, central complex, antennal lobes). The deutocerebrum is elongated laterally and is somewhat flattened anteroposteriorly. The optic lobes flank the brain, with the medulla being lateral to the lobula and lobula plate, and with the lamina occupying the most lateral position. The subesophageal ganglion, which is fused to the brain, is connected posteriorly to the thoracicoabdominal ganglion via the cervical connective. The thoracicoabdominal ganglion is located in the ventral region of the thorax (for a more detailed description of the organization of the adult CNS, see Power, 1943, 1948).

Adult brain—The description of major OA-IR neuronal clusters and neuropil in the adult brain was based on serial histological sections (in frontal and horizontal planes) of whole

mounts processed according to the indirect peroxidase method (see Materials and Methods). In some of the samples, cells with very superficial positions were not easily detected. In Figure 6, we provide a diagram of the adult brain showing the distribution of consistently observed OA-IR neuronal clusters, fibers, and neuropil. In Table 1, we summarize the approximate locations and numbers of the OA-IR neurons.

Six distinct neuronal clusters were detected in the adult brain at different levels along the dorsoventral axis (subesophageal ganglion, esophageal level, and dorsal protocerebrum; Fig. 7). In the subesophageal ganglion, along the midline, a prominent cluster of 12–14 OA-IR neurons was observed (Fig. 7A; SM, subesophageal medial). In some samples, this cluster consisted of three subgroups in the posterior, middle, and anterior subesophageal ganglion. The posterior SM cells occupied more ventral positions than the ones located anteriorly. In frontal sections, the projections of at least some of the SM neurons were detected ascending along the midline towards the ventral part of the esophageal foramen (Fig. 9). All the subesophageal cells showed intense staining and occupied approximately the same positions as the OA-IR cells in the larval subesophageal ganglion.

Dorsal to the SM cluster was the AL (antennal lobe) cluster, composed of four or five bilaterally situated cells located in the deutocerebrum at the level of the esophagus (Fig. 7B). They were close to the midline and presumably corresponded to antennal glomeruli cortical cells. The highly IR AL processes projected posteriorly along the wall of the esophageal foramen.

In the superior protocerebrum, three major OA-IR cell clusters were detected: the dorsal anterior cluster (DAC), the dorsal medial cluster (DMC), and the dorsal posterior cluster (DPC). In frontal sections, the DPC neurons were dispersed in the posterior cortex along the dorsoventral axis. In horizontal sections, the most ventral DPC neurons were detected at the ventral level of the central complex. The DPC cluster consisted of at least six to eight cell bodies on each side of the midline, with some cells in lateral positions (Fig. 7C). The DAC neurons, which consisted of four to five large IR somata per hemibrain, were observed in the anterior cortical margin of the protocerebrum (Fig. 7C). The arrangement of the DAC cell bodies was symmetrical, and the most lateral of the cells were in very lateral positions. The DMC cluster consisted of about four neurons and was localized near the median neurosecretory cells (Fig. 8A).

Finally, two additional IR cells (LP; lateral protocerebrum) were evident in the anterodorsal protocerebrum at the level of the central complex in bilateral positions near the anterior optic tract (Figs. 8A, 9A). Except for the neurons of the subesophageal cluster (SM neurons), which, most likely, persist from the larval stage, all the OA-IR neurons in the adult brain appear to differentiate or start expressing octopamine during metamorphosis.

In addition to the OA-IR neuronal clusters, several IR fibers and neuropil areas were detected in the adult brain. Prominent staining was observed in the components of the central body complex, including the ventral tubercles, the fan-shaped body, and, most intensely, the ellipsoid body (terminology according to Power, 1943; Figs. 8B, 9A). In horizontal sections, OA-IR fiber tracts were detected leaving the central complex between

the fan-shaped body and the ellipsoid body and extended anterolaterally along the anterior optic tracts towards the optic lobes. At approximately the same level, IR bundles originating from posterior lateral positions extended toward the midline beneath the central complex (Fig. 8B).

In the optic lobes, three well-defined layers of OA-IR varicosities were observed. The distal-most layer in the medulla was the most densely stained (Fig. 9A,B). There was also an indication of at least one other more diffuse layer just proximal to the intensely stained distal-most layer (data not shown). The optic lobe neuropil was penetrated by OA-IR fibers from the lateral protocerebrum (Fig. 9B). In horizontal sections, at the level of the esophagus, these fibers appeared to constitute major IR tracts together with IR fibers that connected the anteromedial edge of the medulla and the posterior brain, where they turned to the midline (Fig. 7B). Part of their posterior route can be seen in a frontal section in Figure 8C. The route and location of these fibers suggest that they might be part of the posterior optic tract, which connects the two optic centers. The lamina was devoid of OA-IRy.

Octopamine-IR processes were consistently observed along the esophageal foramen. These bundles appeared to originate from the AL neurons in the antenna1 lobes (Fig. 7B). Finally, two large IR fiber bundles were observed in the posterior cortex of the protocerebrum crossing each other at the midline (Fig. 8C).

Thoracicoabdominal ganglion—The number and distribution of OA-IR neurons in the thoracicoabdominal ganglion was determined from whole-mount and sectioned preparations. OA-IRy was relatively weak in the thoracicoabdominal ganglion, and we have chosen to describe only those neuronal clusters that gave the most reliable and consistent staining. Because background was high, the OA-IR neuronal projections and neuropil were not easily detected.

Octopamine-IR neurons were found in all thoracic and abdominal neuromeres (Fig. 10). All TR somata were located in the ventral midline, and they appeared as single cells or clusters. In the prothoracic neuromere, a single anterior neuron was observed (PTS; prothoracic single), followed by a small cluster of three IR neurons (PTC; prothoracic cluster). In the mesothoracic neuromere, a median row of five or six highly IR neurons (MSC; mesothoracic cluster) was observed. Finally, in the metathoracic neuromere, a cluster of three cells was detected (MTC; metathoracic cluster), followed by a cluster of five to six IR neurons (AC; abdominal cluster) in the midline of the fused abdominal ganglia. In some preparations, two IR fiber tracts were observed projecting from the cervical connective into the thoracicoabdominal ganglion, where they followed a lateral route extending towards the metathoracic neuromere (not shown). Two larger, longitudinal IR fibers were observed between the meso- and metathoracic neuromeres (arrow, Fig. 10A).

DISCUSSION

In this study, we used a specific anti-octopamine antiserum to identify OA-IR neurons in *D. melanogaster* larval and adult CNS and in the larval body wall muscles. Taking into account the sensitivity limitations of immunocytochemical techniques and the fact that we described

only the IRy that was consistently observed, our description probably represents an underestimate of all octopaminergic structures. Technical limitations we encountered were as follows: 1) The background staining in the adult neuropil was high and likely masked many areas of low density IR fibers. 2) The signal in the adult thoracicoabdominal ganglion was weak and background was high. 3) The fixation required to visualize OA-IRy excluded double-labeling studies with other antibodies.

OA-IR pattern

A stereotypic pattern of about 40 OA-IR neurons in the larva and about 70 OA-IR neurons in the adult was revealed by this study. Almost all the cell bodies detected showed strong IRy except for the midline cells (AM) in the larval abdominal ganglia and the LP cells close to the adult optic ganglia, in which the staining was relatively weak. Some of the more noteworthy features of OA-IRy were as follows.

1. OA-IR fibers and varicosities were observed throughout the larval CNS. The distribution of IR somata, however, was restricted and stage specific. The larval brain lobes were devoid of IR somata, whereas neuropil areas and several IR neuronal clusters were detected in the supraesophageal adult brain. These observations suggest that at least some of the adult OA-IR neurons might be born postembryonically and/or differentiate into octopamine-containing neurons during metamorphosis. It has been reported that, in the moth *Munduca sexta*, octopamine biosynthesis is developmentally regulated (Lehman et al., 1993). It is, therefore, conceivable that either the expression of octopamine or the development of some octopaminergic neurons is under hormonal regulation at the pupal stage.
2. OA-IR somata of the larval CNS and many clusters of the adult CNS are located along the midline. The most prominent of these are the SM neurons of the larval and adult CNS. Although we did not follow these neurons during metamorphosis, we suggest, based on their positions and numbers, that they persist through metamorphosis.

The origin and development of midline cells have been studied extensively in *D. melanogaster* (see, e.g.; Klämbt and Goodman, 1991). In particular, the unpaired median neurons have received much attention in several insect species because of their unique morphological and physiological properties (reviewed in Evans, 1985). In locusts, cockroaches, and cricket ventral ganglia, most, if not all, of the peripherally projecting dorsal unpaired median (DUM) neurons contain octopamine in addition to ventrally located unpaired median neurons (VUMs; see, e.g., Eckert et al., 1992; Stevenson et al., 1992). In the abdominal ganglia of *Manduca sexta* larvae and adults, OA-IRy has been detected in two VUMs in the posterior region of each segment that have been compared to the DUMs described in other insects (Pflüger et al., 1993). The AM neurons of the larval ventral ganglion may represent VUM motor neurons projecting into the periphery and innervating the muscles of the body wall. This latter idea is consistent with observations of *D. melanogaster* embryonic VUM neurons, which bifurcate at the midline and innervate several body wall muscles (Sink and Whitington, 1991).

3. The localization of OA-IR cells in the cortex of the antennal lobe (AL cells) suggests a possible involvement of octopamine in olfactory processes. Kreissl et al. (1991) also reported the presence of OA-IR neuronal clusters in median and lateral positions of the antennal lobes of the honeybee, where, according to physiological studies, octopamine is involved in stimulus reinforcement (Bicker and Menzel, 1989).

4. The most prominent neuropil staining is observed in the central complex and in the optic ganglia. The origin of this innervation is not known. In a few samples, a pair of cells was detected close to the anterior optic ganglia at the level of the esophageal foramen. Because these cells were not always observed, they were not included in the description of the OA-IR somata. However, large IR tracts originating from the same area (Fig. 7B) indicate that octopamine probably is contained mostly in axons and in nerve endings and is, perhaps, below the levels of detection in these cell bodies. This possibility may also explain our inability to trace the cellular origin of many axon tracts both in the larva and in the adult (e.g., in posterior protocerebrum; Fig. 8C). Similar observations have been made with choline acetyltransferase in *D. melanogaster* (Gorczyca and Hall, 1987).

The presence of OA-IRy in the optic ganglia and in major fibers that seem to originate from the optic lobe and project towards the brain suggests involvement of octopamine in visual processing. In *Limulus,* a role of octopamine in regulating visual sensitivity has been documented (Kass and Barlow, 1984), and, recently, OA-IRy has been observed in efferent fibers in the lateral optic nerves (Lee and Wyse, 1991).

5. Comparison of the distribution of OA-IR neurons with dopaminergic neurons in the larval CNS shows that both sets have some neurons along the midline of the ventral ganglion (Beall and Hirsh, 1987; Konrad and Marsh, 1987; Budnik and White, 1988; this report). However, there are more octopamine neurons than dopamine neurons. Although the possibility of some colocalization cannot be excluded, we favor the notion that the octopamine and dopamine neurons constitute distinct populations for two reasons: 1) It is unlikely that the antibody cross reacts with an antigen in the dopamine neurons, because the brain lobes, where many clusters of dopamine neurons reside, are completely devoid of OA-IR somata. 2) Octopamine-IR neurons in the ventral ganglion project to the periphery, whereas all dopamine immunoreactive axons are central.

Dopa or dopamine uptake experiments using larval CNSs of *Ddc* mutant (in which the synthesis of dopamine is blocked) and wild type have demonstrated the presence of an extra set of neurons (“novel-CF” neurons) in addition to the normal dopaminergic neurons (Budnik et al., 1986). The location, pattern, and approximate number of the larval octopamine neurons (SM, PM, AM) described in this study resembled that of the “novel-CF” neurons. The possibility that octopaminergic neurons possess the uptake machinery for catecholamines underscores the evolutionary relationships that exist between the various monoamine neurons. Alternatively, this phenomenon may be the result of some lack of specificity of the octopamine uptake system.

Comparison of the OR-IR neuronal pattern to previously characterized 5-HT, FMRF, and proctolin IR neuronal patterns in the larval CNS showed no overlap. However, in the adult brain, FMRF-IR cells have been identified among the neurosecretory neurons of the pars intercerebralis (White et al., 1986), where OA-IR cells are also detected. Whether the same cells contain both molecules or correspond to an heterogeneous population of neurons containing different transmitters has not been determined.

Neuromuscular innervation

OA-IRy was detected in two axons per hemisegment, which exited the CNS, branched over the body wall, and, typically, innervated all but eight muscle fibers per abdominal hemisegment. The OA-IR endings corresponded to type II endings, which can be clearly identified, because they are much smaller than other bouton types and because they span a much larger muscle region, often running both anteriorly and posteriorly along the length of the muscle (Johansen et al., 1989; Budnik and Gorczyca, 1992). It has been previously shown that all type II boutons can be labelled with anti-small synaptic bouton (anti-SSB) antibodies. Our studies of OA-IR endings showed that the muscle-specific pattern of octopamine-containing boutons was very similar to that reported for SSB-IRy. EM studies based on serial sections (Jia et al., 1993) have suggested that type II boutons contain both elliptical dense-core vesicles and small, clear vesicles thought to contain glutamate (Johansen et al., 1989). In other systems, elliptical dense-core vesicles have also been correlated with the presence of octopamine (Lee and Wyse, 1991). In locusts, dorsal unpaired median neurons that contain octopamine also make neurosecretory endings on skeletal muscle (Hoyle et al., 1980). In contrast to OA-IR endings at the fly body wall muscles, however, the locust endings are separated from the muscle fiber by a thick pad of collagenous connective tissue. Physiological studies will be required to determine whether this anatomical difference is physiologically relevant.

Our analysis of muscle fibers innervated by OA-IR boutons showed that there were no segmental differences in abdominal segments 2–7. However, in a few muscle fibers, the innervation by OA-IR boutons was more variable, being absent in a substantial number of cases. Similar variability was also observed using anti-SSB or anti-HRP antibodies to label type II boutons (Budnik and Gorczyca, 1992). These observations suggest that the functional significance of octopamine at the body wall muscles may have muscle fiber specificity. Alternatively, octopamine may be released to the body wall cavity by type II endings, where it could act as a neurohormone in tissues that contain octopamine receptors.

Based on the localization of antigens with putative transmitter/neuromodulator functions at body wall muscle endings and motor neurons, we suggest that body wall motor neurons can be divided into three classes: class I, primarily glutamate containing (type I boutons; Johansen et al., 1989); class II, octopamine and glutamate containing (type II boutons; Johansen et al., 1989; this report); and class III, peptide containing (type III boutons; Anderson et al., 1988; Cantera and Nässel, 1992; Gorczyca et al., 1993). Type I boutons originate from many motor neurons per segment, each of which innervates one to a few muscles (Johansen et al., 1989). type II boutons seem to be derived from two motor neurons per segment that innervate most body wall muscles. Class I and II, therefore, represent a

common innervation feature of most body wall muscles and, therefore, can be presumed to be responsible for most excitatory properties of the body wall muscles. In addition, small subsets of specific muscles are innervated by a few class III, peptide-containing neurons that may have modulatory actions on these muscles. A surprising conclusion derived from these studies is that body wall muscle neuro-muscular junctions are characterized by a remarkable diversity of putative neurotransmitters/neuromodulators. The physiological significance of many of these molecules is not yet understood. However, this diversity suggests that the activity of the body wall muscles is regulated by a complex set of signals.

Our results on octopamine distribution are at variance with those reported in a review by Keshishian et al. (1993). However, in our study, we used three different antioctopamine antisera, and they all stained type II varicosities. This disparity in staining may be the result of using different bleeds (see Materials and Methods) or using different fixation protocols. We have found that neuromuscular junction staining is very susceptible to the concentration and duration of glutaraldehyde fixation.

Future directions

The basic description of the distribution of OA-IRy in *D. melanogaster* is only a first step towards understanding the role of this invertebrate neurotransmitter/modulator/hormone. *D. melanogaster* provides an excellent system for mutational genetic and molecular analysis of neuroactive molecules (reviewed by Restifo and White, 1990; Buchner, 1991). Two *D. melanogaster* mutations, *inactive* and *per*, appear to affect octopamine metabolism (O'Dell et al., 1987; Livingstone and Tempel, 1983). The relationship of these mutations to the octopamine biosynthetic machinery is currently unknown. We have recently cloned a gene candidate for the enzyme tyramine β-hydroxylase, which is required for the conversion of tyramine to octopamine (White and Monastirioti, 1993). We expect that molecular genetic analysis of this locus will facilitate the analysis of octopamine function in *D. melanogaster* and will contribute to the understanding of its role in invertebrates.

ACKNOWLEDGMENTS

We thank Dr. Henning Schneider and Dr. Brigitte Frisch-Brandes for sharing protocols and for fruitful discussions. We also thank Patricia Parmenter, Ed Doherty, and Sarah Stanley for technical assistance. This work was supported by NIH Shared Instrumentation grant RR05615 and NIH grant NS23510 to K.W. and NIH grant NS30072 to V.B.

LITERATURE CITED

Anderson MS, Halpern ME, Keshishian H. Identification of the neurupeptide transmitter proctolin in D. melanoguster larvae: Characterization of fiber-specific neurornuscular endings. J. Neurosci. 1988; 8:242–255. [PubMed: 2892897]

Arakawa S, Goconyne JD, McCombie WR, Urquhart DA, Hall LM, Fraser CM, Venter JC. Cloning, localization. and permanent expression of a D. melanogaster octopamine receptor. Neuron. 1990; 2:343–354. [PubMed: 2156539]

Atwood HL, Govind CK, Wu CF. Neuromuscular junction ultrastructure of ventral longitudinal ahdominal muscles in D. melanogaster larvae. J. Neurobiol. 1993; 24:1008–1024. [PubMed: 8409966]

Beall BJ, Hirsh J. Regulation of the D. melanogaster dopa dccarboxylase gene in neuronal and glial cells. Genes Dcv. 1987; 1:510–520.

Bicker G, Menzel R. Chemical codes for the control of behaviour in arthropods. Nature. 1989; 337:33–39. [PubMed: 2562906]

Braun G, Bicker G. Habituation of an appetitive reflex in the honeybee. J. Neurophysiol. 1992; 67:588–598. [PubMed: 1578245]

Buchner E. Genes expressed in the adult brain of D. melanogaster and effects of their mutations on behavior: A survey of transmitter- and second messenger-related genes. J. Neurogenet. 1991; 7:153–192. [PubMed: 1679453]

Budnik V, Gorczyca M. SB, an antigen that selectively labels morphologically distinct synaptic boutons at the D. melanogaster larval neuromuscular junction. J. Neurobiol. 1992; 23:1054–1066. [PubMed: 1460464]

Budnik V, White K. Catecholamine-containing neurons in D. melanogaster melanogaster: Distribution and development J. Comp. Neurol. 1988; 268:400–413.

Budnik V, Martin-Morris L, White K. Perturbed pattern of catecholamine-containing neurons in mutant D. melanogaster deficient in the enzyme dopa decarboxylase. J. Neurosci. 1986; 6:3682–3691. [PubMed: 3098930]

Budnik V, Zhong Y, Wu CF. Morphological plasticity of motor axon terminals in U. melanogaster mutants with altered excitability. J. Neurosci. 1990; 10:3754–3768. [PubMed: 1700086]

Cantera R, Nässel DR. Segmental peptidergic innervation of abdominal targets in larval and adult dipteran insects revealed with an antiserum against leucokinin I. Cell Tissue Res. 1992; 269:459–471. [PubMed: 1423512]

Crossley, CA. The morphology and development of the D. melanogaster muscular system.. In: Ashburner, M.; Wright, TRF., editors. The Genetics and Biology of D. melanogaster. Vol. 2b. New York Academic Press; 1978. p. 499-548.

David JC, Coulon JF. Octopamine in invertebrates arid vertebrates. A review. Progr. Neurobiol. 1985; 24:141–185.

Downer RGH, Orr GL, Gole JWD, Orchard I. The role of octopamine and cyclic AMP in regulating hormone release from corpora cardiaca of the American cockroach. J. Insect Physiol. 1984; 30:457–462.

Dudai Y, Zvi S. High-affinity [^{3}H]octopamine-binding sites in D. melanogaster melanogaster: Interaction with ligands and relationship to octopamine receptors. Comp. Biochem. Physiol. 1984; 77C:145–151.

Dudai Y, Buxbaum J, Corfas G, Ofarim M. Formamidines interact with D. melanogaster octopamine receptors, alter the flies' behavior and reduce their learning ability. J. Comp. Physiol. A. 1987; 161:739–746.

Eckert M, Rapus J, Nürnberger A, Penzlin H. A new specific antibody reveals octoparnine-like imrnunoreactivity in cockroach ventral nerve cord. J. Comp. Neurol. 1992; 322:l–15.

Evans, PD. Octopamine.. In: Kerkut, GA.; Gilbert, LI., editors. Comprehensive Insect Physiology, Biochemistry and Pharmacology. Pergamon; Oxford: 1985. p. 499-530.

Evans, PD. Molecular studies on insect octopaminc receptors.. In: Pichon, Y., editor. Comparative Molecular Neurobiology. Verlag Birkhauser; Boston: 1992. p. 286-296.

Evans PD, Kravitz EA, Talamo BR, Tunks BG. The association of octopamine with specific neurones along lobster nerve trunks. J . Physiol. 1976; 262:51–70. [PubMed: 792417]

Fields PE, Woodring JP. Octopamine mobilization of lipids and carbohydrates in the house cricket, Acheta domesticus. J. Insect Physiol. 1991; 37:193–199.

D.L., Glanzman.; Krasne, FB. Serotunin and octopamine have opposite modulatoly effects on the crayfish's lateral giant escape reaction. J. Neurosci. 1983; 3:2263–2269. [PubMed: 6415242]

Gorczyca M, Hall JC. Immunocytochemical localization of choline acetyltransferase during development and in Cha^{ts} mutants of D. melanogaster melanogaster. J. Neurosci. 1987; 7:1361–1369. [PubMed: 3106590]

Gorczyca M, Augart C, Budnik V. Insulin-like peptide and insulin-like receptor are localized at neurumuscular junctions in D. melanogaster. J. Neurosci. 1993; 13:3692–3704. [PubMed: 8366341]

Gorczyca M, Phillis RW, Budnik V. The role of tinman, a mesodermal cell fate gene, in axon pathfinding during the development of the transverse nerve in D. melanogaster. Development. 1994; 120:2143–2152. [PubMed: 7925017]

Hidoh O, Fukami J. Presynaptic modulation by octopamine at a single neuromuscular junction in the mealworm (Tenebrio molitor). J. Neurobiol. 1987; 18:315–326. [PubMed: 2885395]

Hoyle G. Neuromuscular transmission in a primitive insect: Modulation by octopamine and catch-like tension. Comp. Biochem. Physiol. 1984; 77C:219–232.

Hoyle G, Coquhoun W, Williams W. Fine structure of an octopaminergic neuron and its terminals. J. Neurobiol. 1980; 11:103–126. [PubMed: 6766495]

Jan LY, Jan YN. Properties of the larval neuromuscular junction in D. melanogaster melanogaster. J. Physiol. 1976; 26:189–214. [PubMed: 11339]

Jia XX, Gorczyca M, Budnik V. Ultrastructure of neuromuscular junctiuns in D. melanogaster: Comparison of wild type and mutants with increased excitability. J. Neurobiol. 1993; 24:1025–1044. [PubMed: 8409967]

Johansen J, Halpern ME, Johansen KM, Keshishian H. Stereotypic morphology of glutamatergic synapses on identified muscle cells of D. melanogaster larvae. J. Neurosci. 1989; 9:710–725. [PubMed: 2563766]

Kass L, Barlow RB. Efferent neurotransmission of circadian rhythms in Limulus lateral eye. I. Octopamine-induced increases in retinal sensitivity. J. Neurosci. 1984; 4:908–917. [PubMed: 6325607]

Keshishian H, Chiba A, Chang TN, Halfon MS, Harkins EW, Jarecki J, Wang L, Anderson MD, Cash S, Halpern ME. Cellular mechanisms governing synaptic development in D. melanogaster melanogaster. J. Neurobiol. 1993; 24:757–787. [PubMed: 8251016]

Klämbt C, Goodman CS. Role of the midline glia and neurons in the formation of the axon commissures in the central nervous system of the D. melanogaster embryo. Ann. N.Y. Acad. Sci. 1991; 633:142–159. [PubMed: 1789544]

Konings PNM, Vullings HGB, Geffard M, Buijs RM, Diederen JHB, Jansen WF. Immunocytochemical demonstration of octopa-mine-immunoreactive cells in the nervous system of Locusta migratoria aud Schistocerca gregaria. Cell Tissue Res. 1988; 251:371–379. [PubMed: 3125977]

Konrad KD, Marsh JL. Developmental expression and spatial distribution of dopa decarboxylase in D. melanogaster. Dev. Biol. 1987; 122:172–185. [PubMed: 3297852]

Kravitz EA. Hormonal control of behavior: Amines and the biasing of behavioral output in lobsters. Science. 1988; 241:1775–1781. [PubMed: 2902685]

Kreissl S, Eichmüller S, Bicker G, Rapus J, Eckert M. Elsner N, Penzlin H. The distribution of octopamine-like immunoreactivity in the brain of the honey bee. Synapse-Transmission. Modulation. Stuttgart: Thieme. 1991:407.

Lee HM, Wyse GA. Immunocytochemical localization of octopamine in the central nervous system of Limulus polyphemus: A light and electron microscopic study. J. Comp. Neurol. 1991; 307:683–694. [PubMed: 1869636]

Lehman HK, Murgiuc C, Hildebrand JG. Developmental regulation of octopamine biosynthesis in the CNS of Manduca serta. Soc. Neurosci. Abstr. 1993; 19:1094.

Livingstone M, Tempe1 B. Genetic dissection of monoamine neurotransmitter synthesis in D. melanogasler. Nature. 1983; 303:67–70. [PubMed: 6133219]

Livingstone M, Schaeffer SF, Kravitz EA. Biochemistry and ultrastructure of serotonergic nerve endings in the lobster: Serotonin and octopamine are contained in different nerve endings. J. Neurobiol. 1981; 12:27–57. [PubMed: 6782192]

Long TF, Murdock LL. Stimulation of blowfly feeding behavior by octopaminergic drugs. Proc. Natl. Acad. Sci. USA. 1983; 80:4159–4163. [PubMed: 16593335]

Malamud JG, Mizisin AP, Josephson RK. The effects of octopamine on contraction kinetics and power output of a locust flight muscle. J. Comp. Physiol. A. 1988; 162:827–835.

Nathanson JA. Octopamine receptors, adenosine 3′,5′-monophosphate, and neural control of firefly flashing. Science. 1979; 203:65–68. [PubMed: 214856]

O'Dell K, Coulon JF, David JC, Papin C, Fuzeau-Braesch S, Jallon JM. La mutation inactive produit une diminution marquee d'octopamine dans le cerveau des Drosophiles. C.R. Acad. Sci. Serie 111. 1987; 305:199–202.

Pflüger HJ, Witten JL, Levine RB. Fate of abdominal ventral unpaired median cells during metamorphosis of the hawkmoth, Manduca sexta. J. Comp. Neurol. 1993; 335:508–522. [PubMed: 8227533]

Power ME. The brain of D. melanogaster melanogaster. J. Morphol. 1943:517–559.

Power ME. The thoracico-abdominal nervous system of an adult insect, D. melanogaster melanogaster. J. Comp. Neurol. 1948; 88:347–409. [PubMed: 18866775]

Restifo LL, White K. Molecular and genetic approaches to neurotransmitter and neuromodulator systems in D. melanogaster. Adv. Insect Physiol. 1990; 22:115–219.

Saudou F, Amlaiky N, Plassat JL, Borrelli E, Hen R. Cloning and characterization of a D. melanogaster tyramine receptor. EMBO J. 1990; 9:3611–3617. [PubMed: 2170118]

Schneider H, Trimmer BA, Rapus J, Eckert M, Valentine DE, Kravitz EA. Mapping of octopamine-immunoreactive neurons in the central nervous system of the lobster. J. Comp. Neurol. 1993; 329:129–142. [PubMed: 8454723]

Siegler MVS, Manley JRPE, Thompson KJ. Sulphide silver stainingfur endogenous heavy metals reveals a subset of dorsal unpaired median neurons in insects. J. Exp. Biol. 1991; 157:565–571.

Sink H, Whitington PM. Location and connectivity of abdominal motor neurons in the embryo and larva of D. melanogaster melanogaster. J. Neurobiol. 1991; 22:298–311. [PubMed: 1909747]

Sombati S, Hoyle G. Generation of specific behaviors in a locust by local release into neuropil of the natural neuromodulatur octopamine. J. Neurobiol. 1984; 15:481–506. [PubMed: 6097645]

Stevenson PA, Pflüger HJ, Eckert M, Rapus J. Octopamine immunoreactive cell populations in the locust thoracic-abdominal nervous system. J. Comp. Neurol. 1992; 315:382–397. [PubMed: 1373157]

Vallés AM, White K. Serotonin-containing neurons in D. melanogaster. melanogaster: Development and distribution. J. Comp. Neurol. 1988; 268:414–428. [PubMed: 3129459]

White K, Monastirioti M. Cloning of a D. melanmgaster gene candidate for tyramine β-hydroxylase. Soc. Neurosci. Abstr. 1993; 19:300.

White K, Hurteau T, Punsal P. Neuropeptide-FMRFamide-like immunoreactivity in D. melanogaster: Development and distribution. J. Comp. Neurol. 1986; 247:430–438. [PubMed: 3088066]

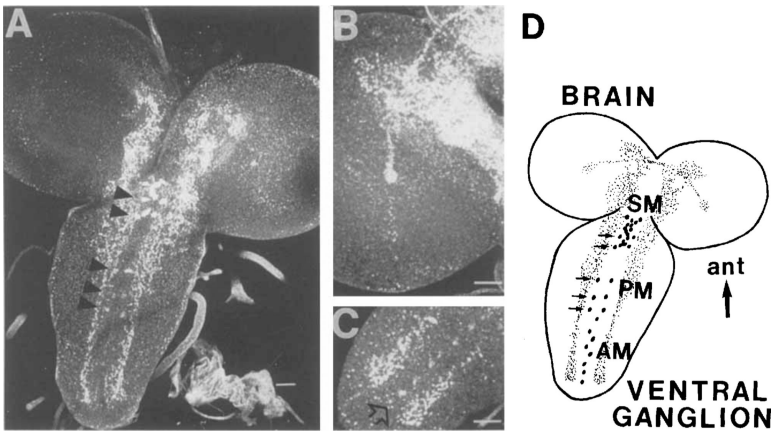

Fig. 1.

Octopamine-immunoreactive (OA-IR) neurons and neuropil in the larval CNS. **A:** Confocal image of the ventral part of the larval CNS showing the OA-IR neurons in the ventral ganglia visualized after immunofluorescent staining. Arrowheads indicate the five PM doublets. Note the intense staining in the neuropil and the immunoreactivity (IRy) extending into the brain lobes. **B:** Note the OA-IRy in the brain lobes and the IR tract that extends laterally ending in a small, highly IR focus. **C:** Note the abdominal ganglion (AM) neurons along the midline of the abdominal ganglia (arrow). **D:** Schematic tracing of the larval central nervous system (CNS) based on whole-mount preparations. Each of the AMs in the drawing represents one or two cells per segment. AM, abdominal medial; PM, paramedial; SM, subesophageal medial; ant, anterior. Scale bars = 25 μm.

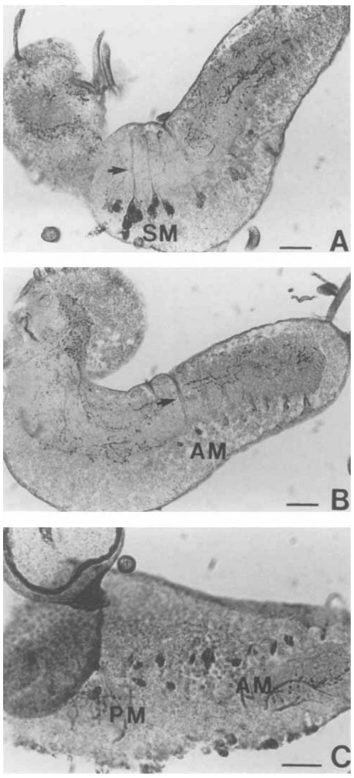

Fig. 2.

Photomicrographs of sections of the larval CNS. Whole-mount samples were processed according to the immunoperoxidase technique and then sectioned. **A,B:** Serial sagittal sections at the midline level showing SM and AM cells. Arrows indicate the IR fibers travelling towards the dorsal neuropil. Note the intensely stained varicosities in the brain lobe and ventral ganglion neuropil. **C:** Horizontal section showing the PM and AM cells. AM, abdominal medial; PM, paramedial; SM, subesophageal medial. Scale bars = 20 μm.

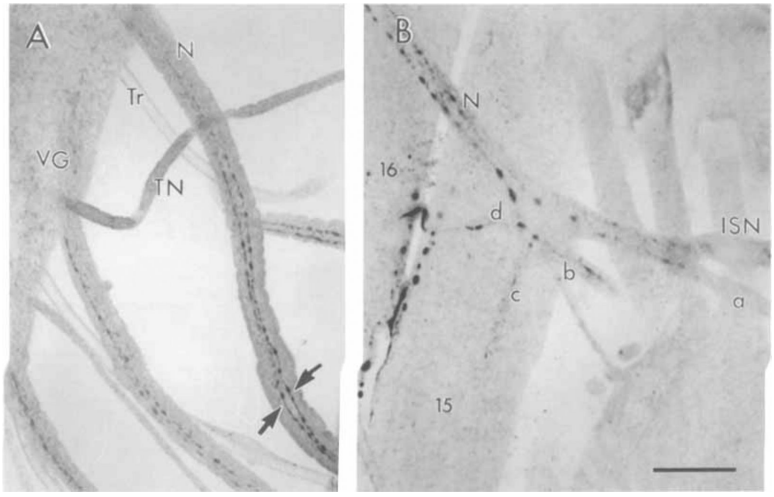

Fig 3.

Confocal image of OA-IRy in larval peripheral nerves. **A:** Two IR fibers (arrows) emerge from the fused segmental and intersegmental nerves. **B:** OA-IRy in these nerves ramify at the body wall musculature. Branches of the segmental nerve are indicated a–d. N, fused segmental and intersegmental nerves; VG, ventral ganglion; TN; transverse nerve; Tr, trachea; ISN, intersegmental nerve. Scale bar = 25 μm.

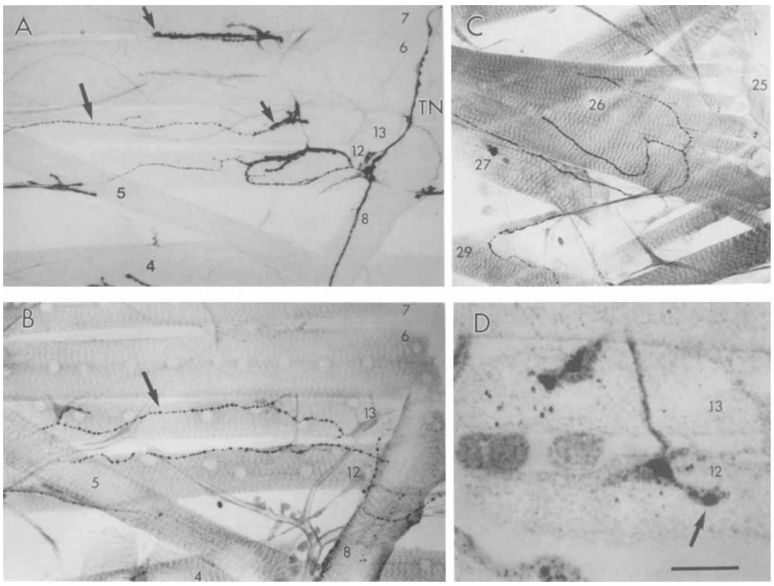

Fig. 4.

Confocal image of OA-1Ry of type II boutons at the body wall muscles. **A:** Antihorseradish peroxidase (anti-HRP) staining of ventral body wall muscles showing all classes of boutons. Note that muscle 6 and 7 contain type I boutons only (short arrow) and are devoid of type II boutons. Muscles 12 and 13 contain both type I boutons and type II boutons (long arrow). **B:** Anti-OA staining showing the same set of muscles as in A (different, sample). Note the correspondence in the distribution of type II boutons (arrow) and OA-IR boutons. **C:** OA-IRy at "deep" muscles 26, 27, and 29. **D:** OA-IRy at muscles 12 and 13 in a first-instar larva less than 20 minutes after hatching. Only a couple of boutons (arrow) are formed at this time. TN, transverse nerve. Scale bar = 75 μm in A,B, 70 μm in C, 6 μm in D.

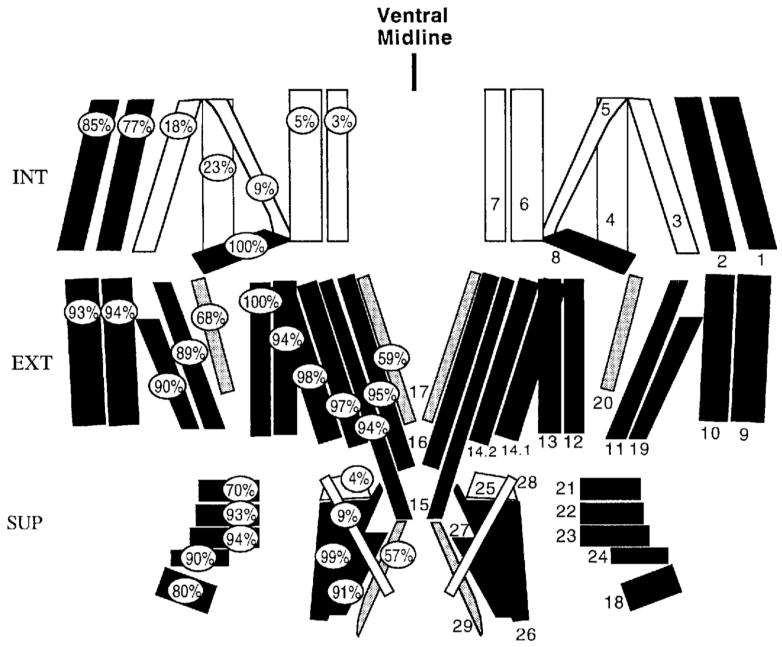

Fig. 5.

Diagrammatic representation of body wall muscles in one abdominal segment (muscle nomenclature, numbers at right) showing the frequency of octopamine expression at each muscle fiber (percentages at left). Color code: black, muscles showing OA-IRy in 70–100% of cases; shaded, 45–69% of cases; white, 0–25% of cases; analysis of 96 hemisegments, eight samples. Body wall muscles were dividcd into three layers for clarity: INT, internal; EXT, external; SUP, superficial.

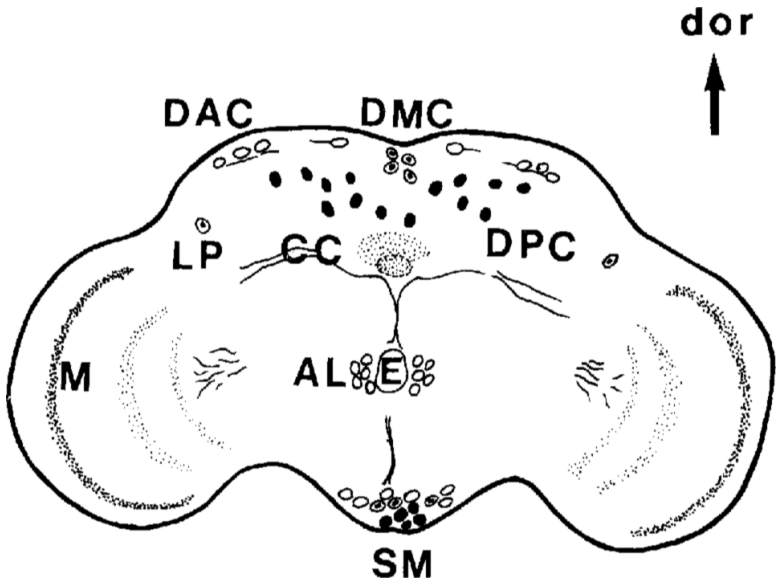

Fig. 6.

OA-IRy in adult CNS. Schematic representation from a frontal view. The approximate position of the OA cell bodies as well as the major IR fibers and neuropil (shaded areas) are indicated. Open circles indicate anteriorly located somata, solid circles indicate posteriorly positioned somata, and circles with a central dot indicate somata that are more central. For description of the individual clusters see Table 1. AL, antennal lobe; DAC, dorsal anterior cluster; DMC, dorsal medial cluster; DPC, dorsal posterior cluster; LP, lateral protocerebrum; SM, subesophageal medial; M, medulla; E, esophagus; CC, central complex; dor, dorsal.

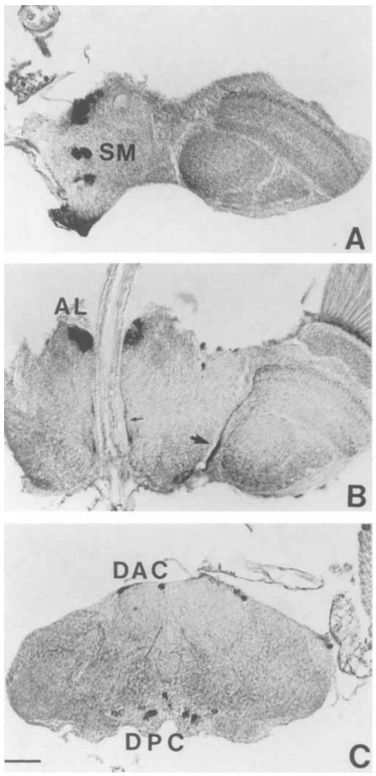

Fig. 7.

OA-IRy in the adult brain visualized with an HRP-conjugated secondary antibody. The photomicrographs present horizontal sections of the adult brain at three levels. **A:** Section of the subesophageal ganglion at the ventral-most level showing some of the SM neurons. **B:** Section at the esophageal level showing both AL cell clustcrs on each side of esophagus. The small arrow indicates part of the IR fibers detected along the esophageal canal. Note the big fiber bundles (large arrow) along the medial boundary of the optic lobe following the route of the posterior optic tract (POT). **C:** Section through the superior protocerebrum at a level showing some neurons of the DAC and DPC clusters. AL, antenna1 lobe; DAC, dorsal anterior cluster; DPC, dorsal posterior cluster; SM, subesophageal medial. Scale bar = 30 μm.

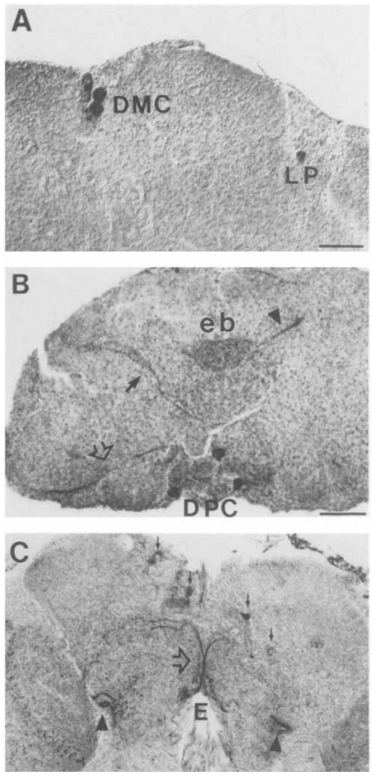

Fig. 8.

OA-IR cells and processes in the adult brain visualized with an HRP-conjugated secondary antibody. **A:** Frontal section at the level of the DMC cells. One of the LP cells is also present. **B:** Horizontal section at the central complex level. Dense IR varicosities are evident in the ellipsoid body (eb). Arrows and arrowhead show the IR fiber bundles detected at this level. Some of the most ventrally located DPC cells are also seen. **C:** Frontal section at a posterior level showing two major IR fibers (open arrow) crossing each other in the midline. Note some of the DPC cells in different focal plane (solid arrnws) and their positions along the ventrodorsal axis. Arrowheads indicate part or the POT fibers in their posterior route (see also Fig. 7B). DMC, dorsal medial cluster; DPC, dorsal posterior cluster; LP, lateral protocerebrum; E, esophagus; eb, ellipsoid body. Scale bars = 20 μm.

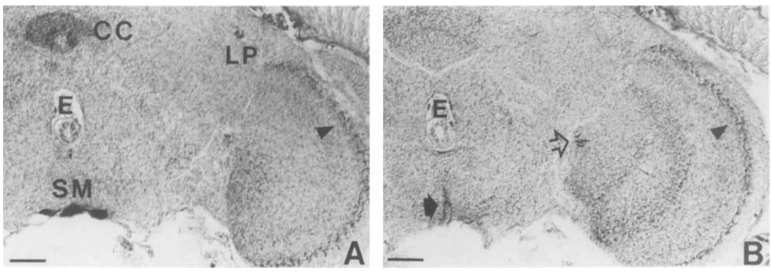

Fig. 9.

Frontal sections showing OA-IRy in the optic lobe. Note the layered organization of IR varicosities in the optic lobes and that the most lateral layer in the medulla (arrowheads, A,B) appears to have the highest density of **OA-IR** varicosities. **A:** Some of the SM cells of the subesophageal ganglion and one of the LP neurons are also present. Note the intense IRy in the central complex (CC) neuropil. **B:** Section in more posterior region than A. Note that the layers of the IR varicosities in the medulla are well defined. Open arrow indicates the incoming IR fibers from the middle brain at the esophagus level (see a horizontal view in Fig. 7B). Solid arrow shows ascending fibers from the SM neurons. LP, lateral protocerehrum; SM, subesophageal medial; E, esophagus; CC, central complex. Scale bar = 20 μm.

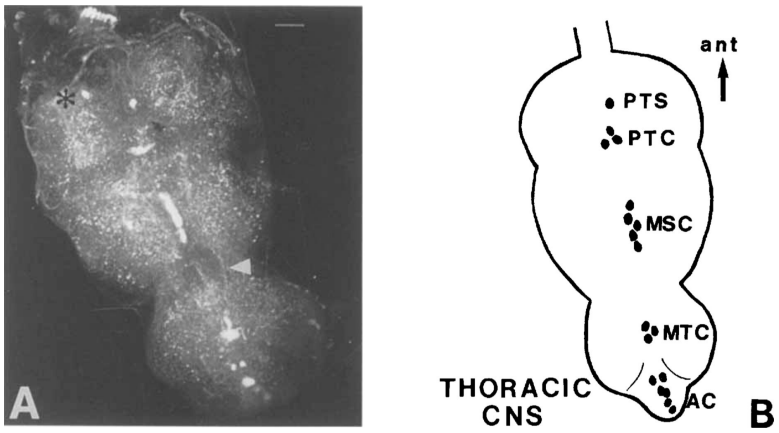

Fig. 10.

A: Confocal image of OA-IRy in the adult thoracic CNS as it is seen in whole-mount preparations after immunofluorescent staining. Arrowhead shows the longitudinal IR fibers observed between meso- and metathoracic neuromeres. Asterisk indicates putative immunoreactive cell that was not consistently detected. **B:** Schematic representation of the OA-IR neuronal somata in the thoracic CNS. AC, abdominal cluster; MSC, mesothoracic cluster; MTC, metathoracic cluster; PTC, prothoracic cluster; PTS, prothoracic single; ant, anterior. Scale bar = 25 μm.

TABLE 1

Position of Octopamine-Immunoreactive Neuronal Clusters in Adult CNS

Group	No. of cell bodies	Location
DAC[1]	4–5	Dorsal protocerebrum, anterior marginal sites
DMC	4	Dorsal medial protocerebrum, region of the median neurosecretory cells
DPC	~15	Dorsal protocerebrum, sites extending in different levels in posterior cellular rind
LP[1]	1	Lateral protocerebrum, dorsal level of central complex, close to anterior optic tract
AL[1]	4–5	Ventral brain at the esophagus level very close to midline
SM	12–14	Midline cells with sites extending anterior to posterior subesophageal ganglion both in larval and adult CNS
PTS	1	Single cell in midline of prothoracic neuromere
PTC	3	Cell cluster in midline of prothoracic neuromere
MSG	5–6	Midline cell cluster in mesothoracic neuromere
MTC	3	Midline cell cluster in metathoracic neuromere
AC	5–6	Cell cluster in the adult fused abdominal ganglia
PM	10	Five pairs of neurons flanking the midline of larval subesophageal and thoracic ganglia
AM	1–2/segment	Ventral medial neurons in the abdominal ganglion of larval CNS

[1]Number of cells per hemibrain.